ANL/ET/RP-96422

PRACTICAL SUPERCONDUCTOR DEVELOPMENT FOR ELECTRICAL POWER APPLICATIONS

ARGONNE NATIONAL LABORATORY

QUARTERLY REPORT FOR THE PERIOD ENDING MARCH 31, 1998

This is a multiyear experimental research program focused on improving relevant material properties of high-T_c superconductors and on development of fabrication methods that can be transferred to industry for production of commercial conductors. The development of teaming relationships through agreements with industrial partners is a key element of this program.

Technical Highlights

Recent work on microstructural development and current distribution in Bi-2223 powder-in-tube (PIT) tapes, grain-boundary studies, and a novel application for high-temperature (high-T_c) superconductors are discussed.

Phase and Microstructural Development in Ag/Bi-2223 Conductors

By increasing the sintering temperature of Bi-2223 PIT samples 20-25°C, to near the Bi-2223 stability limit, we have increased J_c from 1 to 10 kA/cm^2 for samples with a Pb content of $Pb_{0.20}$ and from ≈6 to 15 kA/cm^2 for samples with a Pb content of $Pb_{0.25}$. For samples with higher Pb content (≥$Pb_{0.30}$), an increase in the sintering temperature raised J_c only modestly (≈5-10%), despite noticeably increasing density and improving grain alignment. Microscopy showed that impurity phases in samples processed at the higher temperatures tended to spread in thin layers along the Bi-2223 grain boundaries. With this type of morphology, a small amount of impurity phase can cover a large portion of the Bi-2223 grain boundaries and significantly affect performance. Therefore, minimizing second-phase content may be crucial to realizing improved connectivity from the higher density and better grain alignment that result from processing near the Bi-2223 stability limit.

One reason that second phases are present in Bi-2223 tapes may be that the overall composition of the tape does not lie within the Bi-2223 single-phase field. When the composition of Bi-2223 grains in fully processed tapes was measured by energy-dispersive analysis of X-rays, we found that our standard composition, $Bi_{1.8}Pb_{0.3}Sr_{2.0}Ca_{2.0}Cu_{3.1}O_x$, was slightly rich in calcium and copper relative to the composition of the Bi-2223 grains. Therefore, in an attempt to reduce the second-phase content of our Bi-2223 tapes, calcium- and copper-deficient Bi-2223 powders were prepared. The compositions of the powders, determined by inductively coupled plasma-atomic emission spectroscopy (ICP-AES), are shown in Table 1.

DISCLAIMER

Although Powder 1 was intended to have our standard composition, and serve as our reference, ICP-AES showed that it was in fact slightly calcium- and copper-deficient relative to the standard composition. Powders 2 and 3 were progressively more deficient in calcium relative to Powder 1, whereas Powders 4 and 5 were deficient in copper. Monofilament PIT tapes were made from each of the powders, and then short lengths (≈3 cm) of tape were heat treated over a range of temperatures. The microstructures of heat-treated tapes were examined by scanning electron microscopy (SEM) to identify the composition and overall concentration of impurity phases. Critical current density (J_c) was also measured.

Table 1. Composition of Bi-2223 powders in terms of stoichiometric coefficients, as determined by ICP-AES

Sample Number	Bi	Pb	Sr	Ca	Cu
1	1.83	0.28	1.97	1.91	3.00
2	1.85	0.27	1.97	1.83	3.00
3	1.85	0.27	1.97	1.76	3.00
4	1.83	0.27	1.98	1.90	2.95
5	1.84	0.26	1.96	1.90	2.88

The Bi-2223 powders were prepared by first making Pb-doped 2212 powders, $Bi_{1.8}Pb_{0.3}Sr_{2.0}Ca_xCu_yO_8$, where the calcium content x varied from 0.76 to 0.91 and the copper content y varied from 1.88 to 2.00. Powder mixtures with appropriate amounts of Bi_2O_3, PbO, $SrCO_3$, $CaCO_3$, and CuO were calcined first at reduced total pressure of ≈400 Pa O_2 (20°C/h to 750°C, followed by 6 h at 750°C) to ensure complete decomposition of the carbonates. After calcining at reduced pressure, the Bi-2212 phase was formed by further calcining for 24 h at 840°C in CO_2-free air at ambient pressure. The powders were then ball milled in isopropyl alcohol for 12-16 h and calcined again for 24 h at 840°C in CO_2-free air at ambient pressure. Calcinations in ambient air were repeated with intermediate ball milling until near-single-phase materials were obtained. X-ray analysis showed that Bi-2212 was the dominant phase in each of the powders, but the most calcium- and copper-deficient compositions also contained small amounts of Bi-2201. Bi-2223-precursor powders were prepared by mixing each of five Pb-2212 powders with an equimolar amount of $CaCuO_2$, then ball milling in isopropyl alcohol for 12-16 h and calcining at ≈400 Pa (60°C/h to 720°C, followed by 3 h at 720°C) to eliminate carbon introduced by milling. PIT tapes were prepared from the Bi-2223-precursor powders.

Samples (≈3 cm long) were cut from the tapes and heat treated in 8% O_2 in the temperature range of 823-850°C. Thermomechanical processing of the tapes began by annealing for 50 h at the chosen heat–treatment temperature, after which the

tapes were uniaxially cold pressed at ≈2 GPa. Following pressing, the tapes were annealed for an additional 100 h at the selected heat-treatment temperature. The process of pressing and then annealing was repeated until cumulative heat-treatment times of 250 h had been reached. The J_c of each tape was measured at 77 K in zero applied field with a 1 μV/cm criterion and the four–probe method.

Figure 1 shows J_c as a function of temperature for samples heat treated in 8% O_2 for 250 h with two intermediate pressings. These data are for tapes made from Powder 1, but tapes made from the other powders showed similar trends. The sharp decrease in J_c above 842°C suggests that Bi-2223 may be partially decomposing above this temperature. X-ray diffraction patterns from tapes annealed at ≥846°C show the presence of Bi-2201, a finding that indicates partial melting of Bi-2223. The increase in J_c up to 842°C is consistent with earlier results, which showed that Bi-2223 is stable in tapes in 8% O_2 up to ≈845°C. As in the earlier study in which our standard composition was used, the density increased, grain alignment improved, and size of second-phase particles increased from <5 mm to 5-10 mm as heat-treatment temperature increased from 822 to 842°C.

Figure 2 shows J_c values of the five compositions after processing for 250 h in 8% O_2 at 842°C; J_c is plotted as a function of calcium or copper deficiency relative to Powder 1, whereas Powder 1 represents "zero" deficiency. J_c drops significantly when either the calcium or copper content is decreased relative to Powder 1. These results may suggest that decreasing the calcium and/or copper content of Bi-2223 powder is not beneficial in terms of J_c or phase purity; however, it should be remembered that Powder 1 was itself deficient in calcium and copper relative to our standard composition. Preliminary examination by SEM qualitatively shows that the amount of second phase in the tapes increases as the composition becomes more deficient in either calcium or copper. In the future, the amount of second phases will be quantified and the second phases will be catalogued. In addition, compositions with calcium and copper contents between those of our standard composition and the composition of Powder 1 may be prepared and tested.

Imaging Raman Microscopy for Exploring Phase Evolution in Superconductors

Raman microspectroscopy and imaging Raman microscopy have proved to be powerful tools for studying the evolution and spatial distribution of chemical phases in the bismuth-based (BSCCO) and thallium-based (TBCCO) families of high-T_c superconducting ceramics. These techniques have been applied to compressed/sintered powders and silver-clad composite conductors in conjunction with SEM and energy-dispersive X-ray spectroscopy. Many important insights have been gained about the identity, size, shape, orientation, and spatial distribution of the various nonsuperconducting secondary phases (NSPs) that form and dissipate during heat treatment of the silver-clad BSCCO and TBCCO composite tapes.

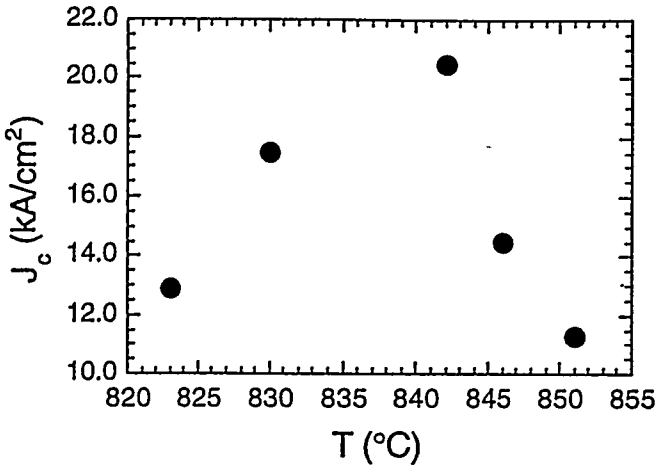

Fig. 1.
J_c at 77 K vs. temperature for $Bi_{1.83}Pb_{0.28}Sr_{1.97}Ca_{1.91}Cu_{3.00}O_{10+\delta}$ (the reference composition) heat treated in 8% O_2 for 250 h with two intermediate pressings.

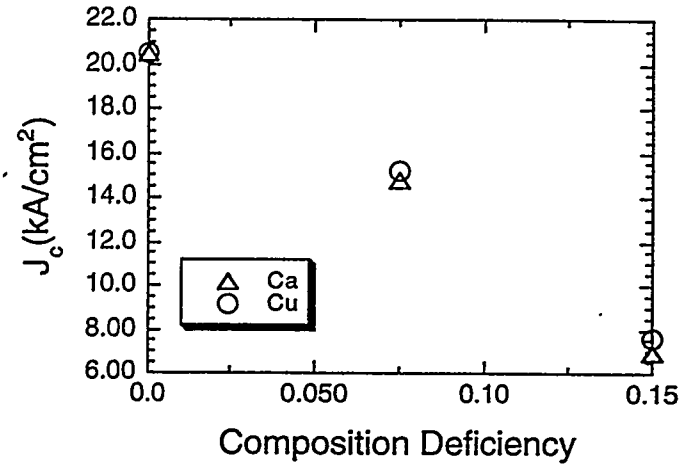

Fig. 2.
J_c at 77 K versus calcium deficiency and copper deficiency relative to reference composition $Bi_{1.83}Pb_{0.28}Sr_{1.97}Ca_{1.91}Cu_{3.00}O_{10+\delta}$. Samples were heat treated for 250 h in 8% O_2 at 840°C, with two intermediate pressings.

The results have allowed us to determine key mechanistic features that control/influence the formation of the superconducting phases as heat treatment progresses, including the location of Pb-rich NSPs and the identification of the constituent phases in certain NSP agglomerations that tend to resist dissipation as high-T_c phase formation proceeds to completion. Results of recently completed studies on three different types of samples are summarized below.

1. Investigation of Ag/Tl-1223 Composites with Tl + Bi + Pb = 1.1

In a published study that employed magnetization and X-ray diffraction methods, we reported some observations concerning the influence of bismuth substitution on liquid formation in heavily strontium-doped Ag/Tl-1223 composite conductors. An extension of this study that included samples doped with both bismuth and lead produced a series of samples that we have investigated by RMS and IRM. For this particular series of samples the ceramic powder stoichiometry was $Tl_aBi_bPb_cBa_{0.4}Sr_{1.6}Ca_{2.0}Cu_{3.0}O_x$, where $a + b + c$ was kept at a value of 1.1. Three composite wires with varied thallium and bismuth content, and two wires with varied thallium, bismuth, and lead content were heat treated at 840°C for 20 h in

0.08 atm O_2. Specimens from all five wires were mounted in epoxy, polished, and examined by the two Raman microscopy techniques to determine phase content. The remaining segments of the five wires were subjected to a second heat treatment at 870°C for 0.2 h in 0.08 atm O_2 and they too were examined by Raman microscopy. The compositions and liquidus onset temperature (i.e., mp as determined by differential thermal analysis) of each of the five Ag/Tl-1223 composites are listed in Table 2.

Table 2. Summary of $(Tl,Bi,Pb)_{1.1}Ba_{0.4}Sr_{1.6}Ca_{2.0}Cu_{3.0}O_x$ RMS results

Tl/Bi/Pb (mp)	Heat Treatment I (840°C)	Heat Treatment II (870°C)
0.9/0.2/0.0 (863°C)	Tl-1223, Sr-2/1, Ca-2/1, 14/24, Y	Tl-1223, Sr-2/1, Ca-2/1 (minor 14/24, Y, and CuO)
0.7/0.4/0.0 (865°C)	Tl-1223, Sr-2/1, Ca-2/1, 14/24, Y (minor CuO and Z)	Tl-1223, Sr-2/1, Ca-2/1, 14/24, (minor CuO and Z)
0.5/0.6/0.0 (849°C)	Tl-1223, 14/24, Y (minor Ca-2/1)	Tl-1223, Ca-2/1, 14/24, Y (minor CuO)
0.5/0.3/0.3 (847°C)	Tl-1223 (minor Sr-2/1 and Ca-2/1)	Tl-1223, Ca-2/1, 14/24 (minor CuO, Y)
	Tl-1223 (minor Ca-2/1)	Tl-1223, Ca-2/1, 14/24
0.3/0.4/0.4 (831°C)	--	--

The two heat-treatment temperatures, 840 and 870°C, were chosen to be slightly below and slightly above the range of liquidus onset temperatures for the five wires, with recognition that the liquidus onset temperature for the 0.3/0.4/0.4 wire is an exception. Raman spectra of the six phases that were repeatedly observed in the five wires after Heat Treatment I and after Heat Treatment II are shown in Fig. 3. The three spectra on the right are known from our prior work to be those of calcium-rich $(Ca,Sr)_2CuO_3$ (Ca-2/1), strontium-rich $(Ca,Sr)_2CuO_3$ (Sr-2/1), and $(Ca,Sr)_{14}Cu_{24}O_{41}$ (14/24). The three on the left (from top to bottom) are those of (a) Tl-1223, (b) a phase we refer to as the "Y" phase and that contains many of the features found in Raman spectra of monoclinic forms of $BaBiO_3$ and metal-substituted versions thereof, and (c) an as-yet-unidentified phase (or collection of phases) we observed in minor amounts in two specimens and that we call the "Z" phase. A compilation of the phases we found with regularity in each of the five Ag/Tl-1223 composites after the first and second heat treatments is included with the information in Table 2.

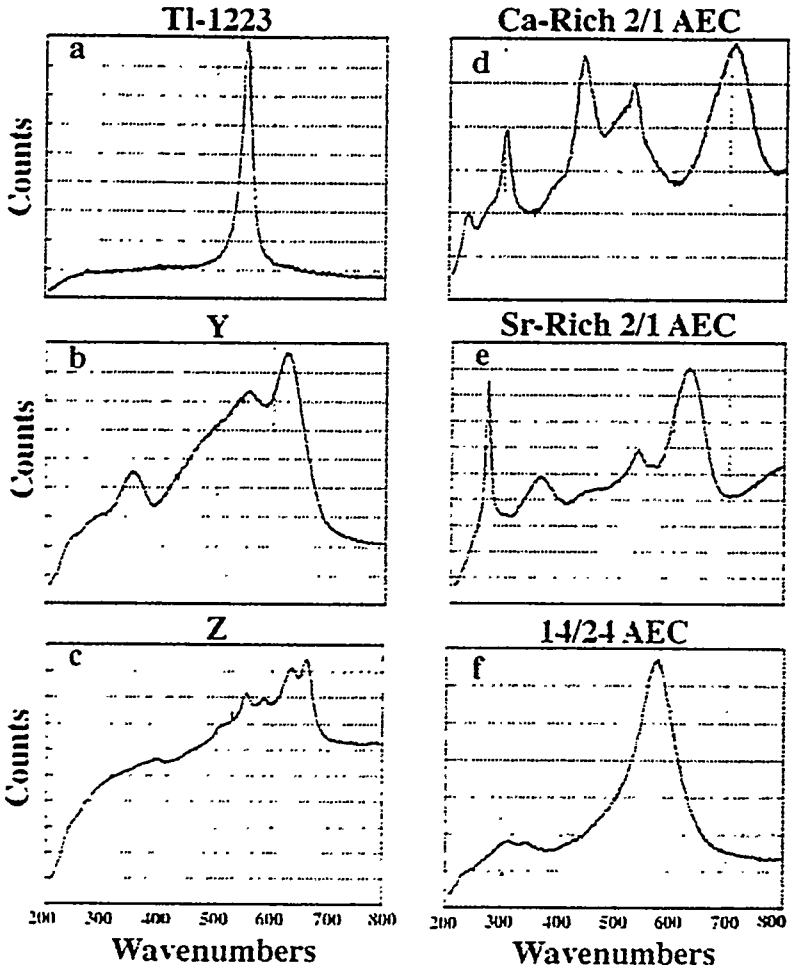

Fig. 3. Spot-focused Raman spectra of six phases seen repeatedly in bismuth- and bismuth + lead-doped Ag/Tl-1223 samples after heat treatment at 840 and 870°C in 0.08 atm O_2; (a-c) current work, (d-f) our previous work.

The results in Table 2 give evidence of several possible links between Tl/Bi/Pb stoichiometry and phase chemistry and between heat-treatment temperature and second-phase content. Increasing bismuth (decreasing thallium) in the absence of lead caused an increase in the $BaBiO_3$-like Y phase and a decrease in the Sr-2/1 phase. The introduction of lead seemed to cause a decrease in the Y and Sr-2/1 phases and a general decrease in the overall second-phase content. CuO, although always present in minor amounts, was more prevalent in the samples that were subjected to the higher heat treatment temperature, i.e., samples that very likely incurred at least partial melting.

Many of the nonsuperconducting second phases observed in this particular series of Tl-1223 wires were 10 μm or larger and thus they appeared to disrupt the connectivity of the superconducting grains. An example of this is shown in Fig. 4, where we have collected Raman images of a large Ca-2/1 crystallite and adjacent patches of Tl-1223. The defocused Raman spectrum in the extreme left of Fig. 4a was obtained from the circled area in the white-light image (Fig. 4b). Bands A, B, C, and E belong to the Ca-2/1 phase. Background-corrected Raman images of Band B (B/B2 in Fig. 4) and Band E (E/B5 in Fig. 4) highlight the location of the Ca-2/1 phase. (Bands A and C are images that are similar to B/B2 and E/B5.) Band D in the defocused spectrum belongs to Tl-1223 and its background-corrected Raman image is shown as D/B4 in Fig. 4. The Raman images show how the large Ca-2/1 crystallite intrudes on the connectivity of two grains of Tl-1223. Large nonsuperconducting second-phase particles, a persistent problem in silver-sheathed composite conductors, are being studied at many levels in the high-T_c superconductor community.

2. Phase Assemblages in a Fully Processed Ag/Bi-2223 Wire-in-Tube Composite

Wire-in-tube (WIT) type Ag/Bi2223 composites are prepared by positioning a thick silver wire along the centerline of a silver billet, packing Bi-2223 precursor powder around the thick wire so that it fills the inside of the billet, capping and drawing the billet into a fine wire, rolling the wire into a flat filament, and heat treating the filament to form the Bi-2223 phase. This approach produces a concentric silver/ceramic/silver laminate in which the ceramic ring is only a few micrometers thick in some places. The impetus for such an embodiment is the mounting evidence that most of the supercurrent in an Ag/Bi-2223 composite wire is carried by a thin, well-textured layer of Bi-2223 next to the silver sheath. According to at least one group of investigators, Ag/Bi-2223 composite conductors prepared by the WIT technique exhibit J_c values that are among the highest reported for BSCCO-based wires at 77 K. The stoichiometry of the particular specimen reported in this paper was $Bi_{1.8}Pb_{0.35}Sr_{2.0}Ca_{2.0}Cu_{3.0}O_y$. The specimen was heat treated for 250 h at 840°C in 0.08 atm O_2, with intermediate pressing after the first 50 h and a second pressing after 100 h, and then slow cooled (10°C/h to 700°C, then 60°C/h to room temperature). We used Raman microspectroscopy to identify phases near the ceramic/silver interfaces and in regions of the ceramic that were farthest from the silver surfaces.

The white-light image in Fig. 5 shows the longitudinal view of a segment of ceramic core running between the silver sheath and the central silver wire (at this point flattened by the rolling process to a narrow elliptical ribbon shape). This particular segment is in the flattened middle portion of the wire where the ceramic layer is thinnest. Raman spectra, obtained with the laser spot-focused to a

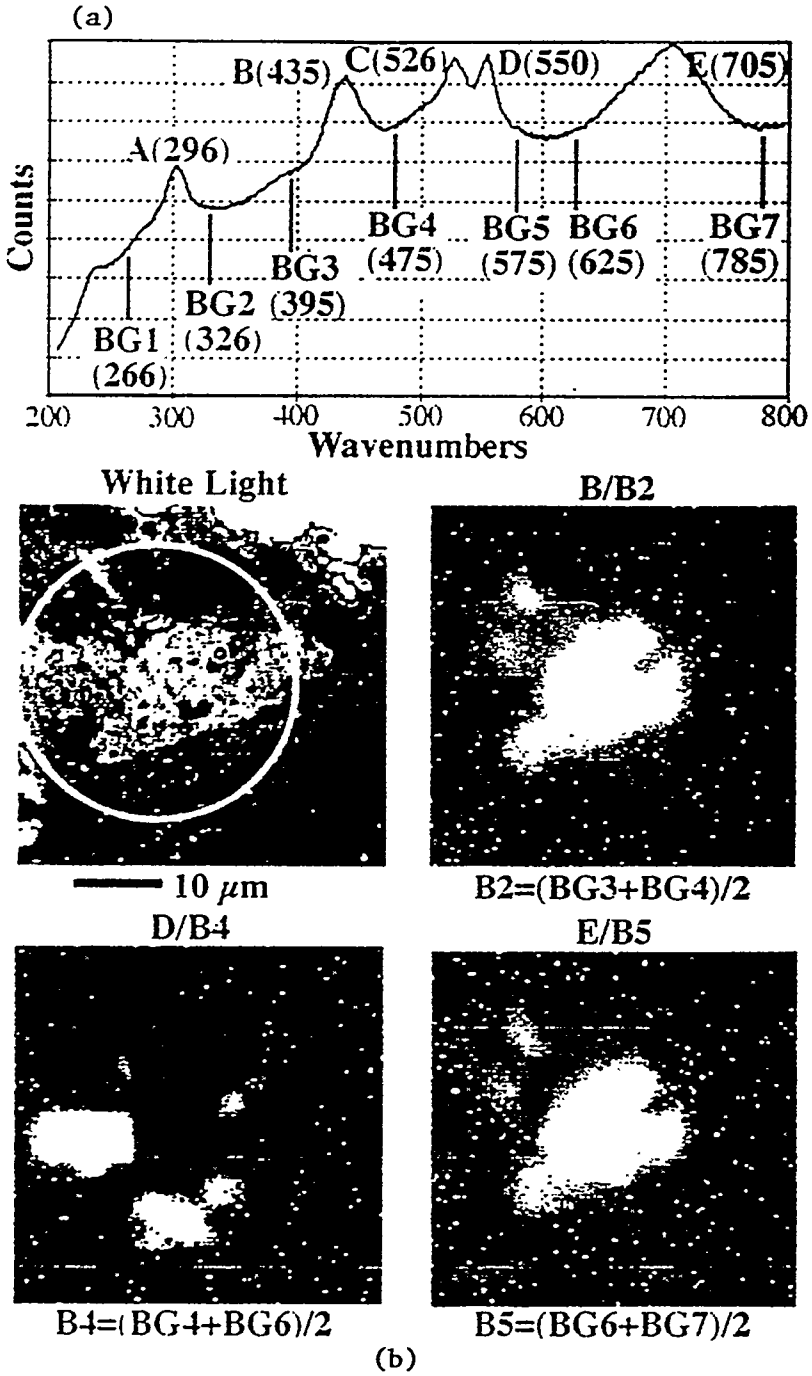

Fig. 4. Imaging Raman microscopy analysis of large calcium-rich 2/1 alkaline earth cuprate crystallite in bismuth-doped Ag/Tl-1223 specimen heat treated at 870°C in 0.08 atm O_2. (See text for description of details.)

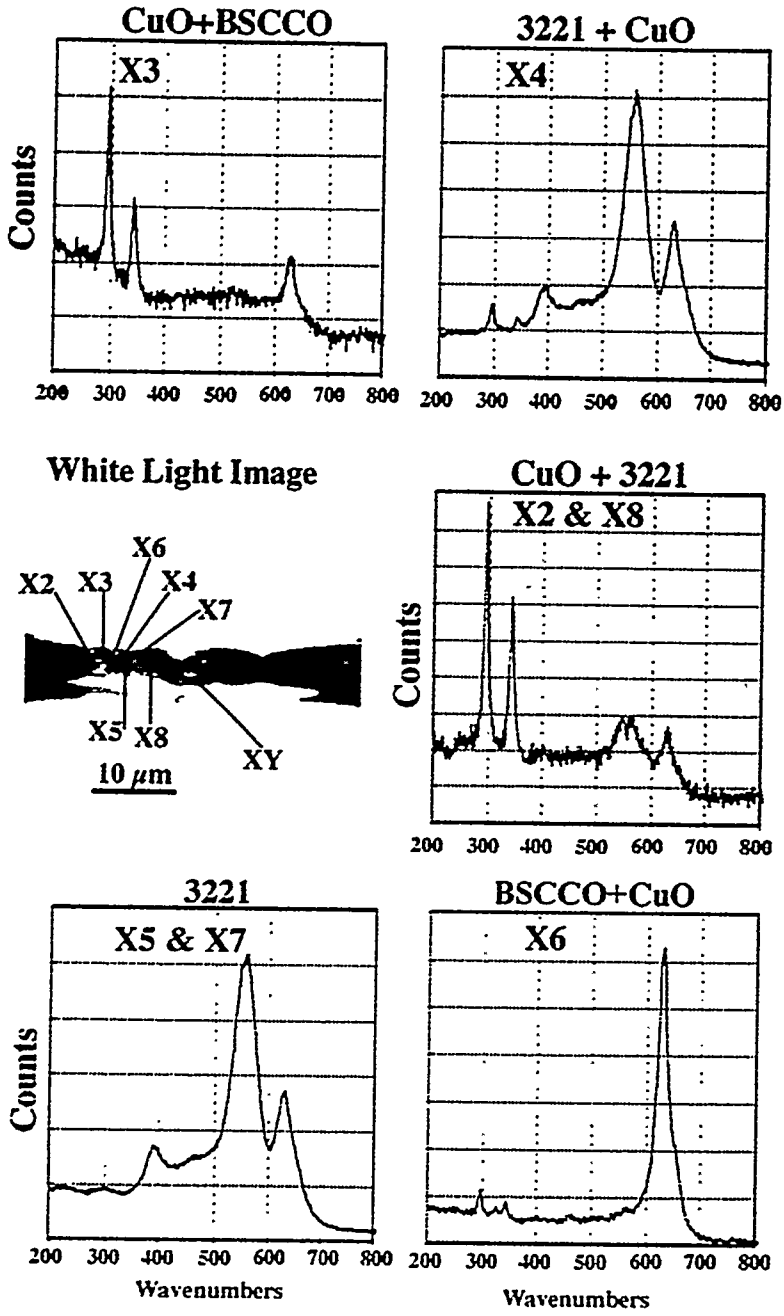

Fig. 5. Spot-focused Raman spectra near ceramic/silver interface in fully-processed WIT-type Bi-2223 composite conductor, showing occurrence and spatial distribution of CuO, 3221, and Bi-2212/Bi-2223.

1-2-μm diameter, reveal a phase mix in this thinned region that consists mostly of Bi-2223/Bi-2212 (each with a band at ≈625 cm^{-1}), copper oxide (bands at 300 and 350 cm^{-1}), and $(Bi,Pb)_3Sr_2Ca_2Cu_1O_w$ (also known as the 3221 phase with bands at ≈620, 555, and 395 cm^{-1}), with the indicated band assignments being guided by our prior studies of well-characterized standards.

In transverse views of this same WIT composite, there are regions of the ceramic material in the corners of the filament near the ends of the flattened center wire that are more than 10 m from any silver surfaces. The white-light image of one such region is shown in Fig. 6, together with a defocused Raman spectrum of the circled area in the white-light image. Background-corrected Raman images of bands A and B in the defocused spectrum are shown in the middle of Fig. 6. Spot-focused spectra, taken in the heart of Band-A and Band-B image emanations (spots X and Y in the white-light image) reveal the presence of the Ca-rich 2/1 alkaline earth cuprate and Bi-2223/Bi-2212, respectively. The key finding from the results in Figs. 5 and 6 is that the second-phase compositions in regions close to and distant from the silver differ. The 3221 phase, which has been linked to higher critical currents and enhanced flux pinning in Ag/Bi-2223 composites and which is known to be more prevalent in slow-cooled specimens (as is the case for the subject WIT sample), is readily detected in regions of the ceramic that are near the silver, but is not detected in ceramic material ≥10 μm away from any silver surfaces. This is the first evidence we have uncovered to suggest that 3221 formation may be connected with proximity to silver.

3. Second-Phase Congestion in PIT-Type Ag/Bi-2223

One of the most informative uses of IRM in our work has occurred during our efforts to elucidate the influences of lead on the formation and stabilization of the Bi-2223 phase in Ag/Bi-2223 composite conductors. One important finding has been that two common second phases in such composites, copper oxide and alkaline earth plumbate, tend to appear close to one another, and the principal conclusion we have drawn from this observation is that they do not react with one another under the heat-treatment conditions normally used to process Ag/Bi-2223 wires. An example of the type of data that support this conclusion is given in Fig. 7.

The defocused Raman spectrum in Fig. 7 (upper right inset) was obtained from the circled area in the white-light image (upper left inset). From our prior work, we can preliminarily identify Raman Bands A, B, and C in the defocused spectrum as being associated with copper oxide, alkaline earth plumbate, and Bi-2223/Bi-2212. Raman images of each of these bands (shown in the middle of Fig. 7) reveal the locations within the interrogated region (circled area in the white-light image) from whence each band is emanating. The intensity of Band A relative to its local average background (B1) in the defocused spectrum is at the limit of imagable

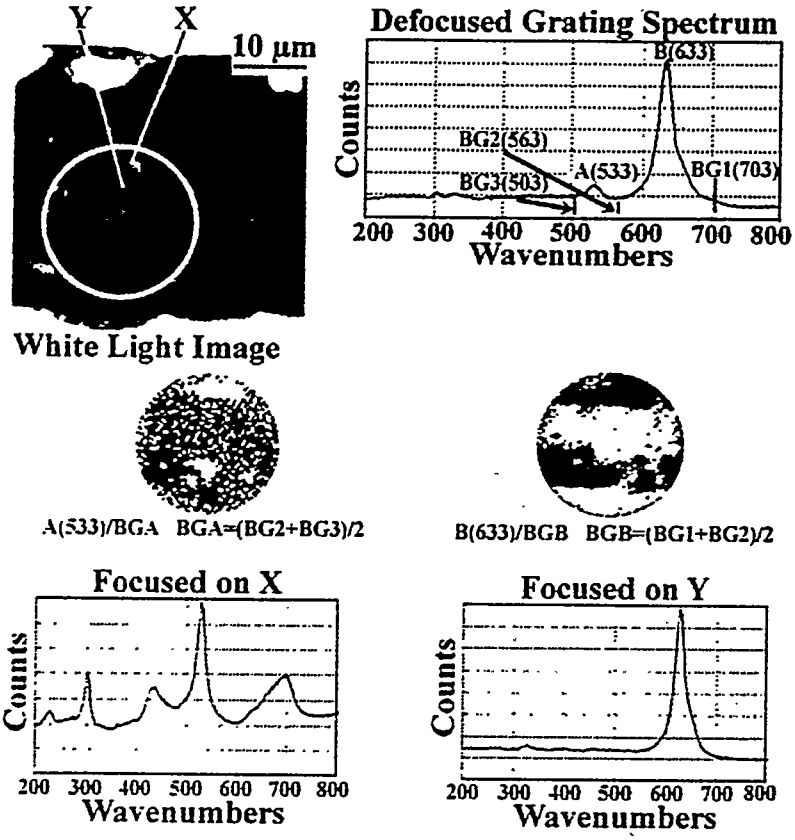

Fig. 6. Imaging Raman microscopy analysis of interior region of ceramic core in same full-processed Ag/Bi2223 composite under study in Fig. 3. Here, coexisting phases are calcium-rich 2/1 alkaline earth cuprate and Bi-2212/Bi-2223. (See text for description of details.)

values, but the Band A scattering appears to be coming primarily from the large crystallite in the center of the white-light image. We know from energy dispersive X-ray analysis performed in a scanning electron microscope that the only metallic element present in this crystallite is copper. The spot-focused Raman spectrum of location "X" in the white-light image, shown as the lower-left inset in Fig. 7, confirms the presence of copper oxide as the dominant phase, especially because we have found copper oxide to be a relatively poor Raman scatterer in the many BSCCO specimens we have examined.

It is also apparent in the B/B2 Raman image in Fig. 7 that the regions of the interrogated area that are producing Band-B scattering surround the copper oxide crystallite. The spot-focused Raman spectrum of location Y in the white-light image, which is in the heart of the imaged Band B emanation, is unequivocally that

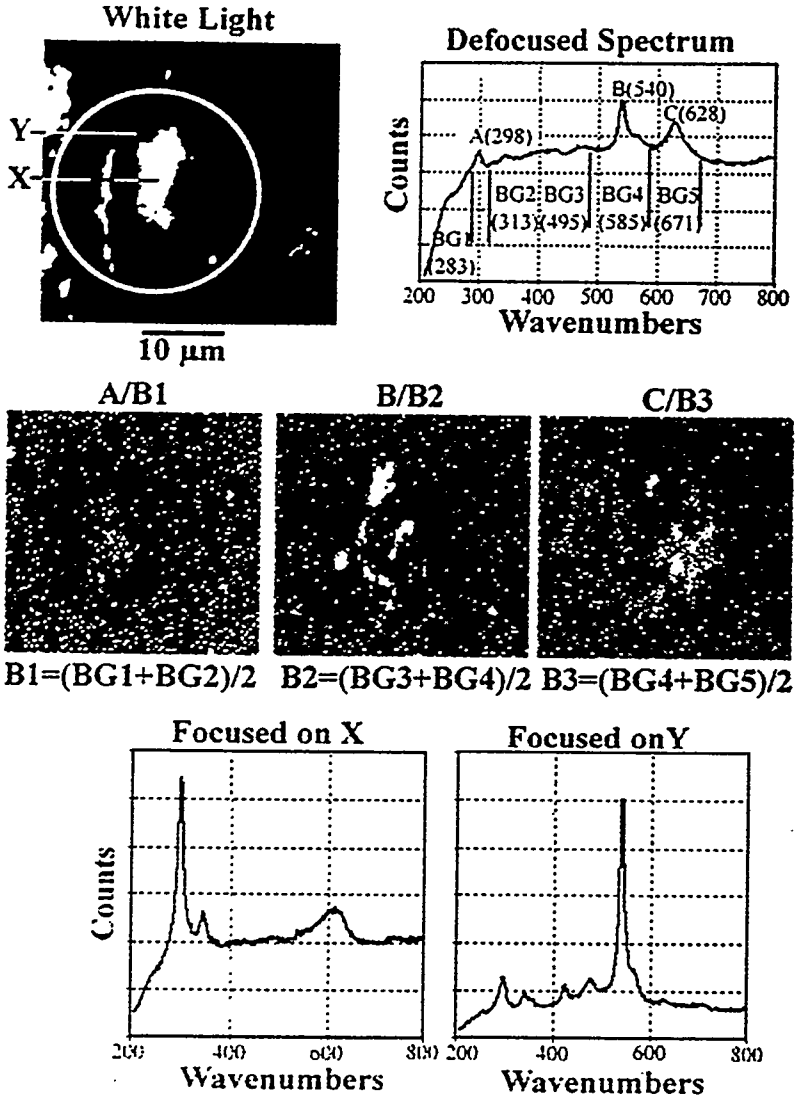

Fig. 7. Imaging Raman microscopy analysis of region of CuO + Ca_2PbO_4 congestion in Ag/Bi-2223 monofilamentary composite conductor.

of Ca_2PbO_4. This type of CuO/plumbate congestion is observed with regularity in fully-processed versions of slow-cooled and/or lead-rich Ag/Bi-2223 composites. The desire to eliminate this congestion has led Ag/Bi-2223 wire manufacturers to consider modification of stoichiometry and powder preparation specifications. Notice also that one can locate the adjacent Bi-2223/Bi-2212 regions by imaging Band C in the defocused Raman spectrum of Fig. 7. Image C/B3 shows how the CuO/plumbate congestion could be acting to terminate grain growth of the superconducting phase.

Critical Current Density of Bicrystal Grain Boundaries

Thin-film, [001] tilt, bicrystal grain boundaries in $YBa_2Cu_3O_7$ (Y-123) indicate that J_c is a strong function of misorientation angle θ between the two bicrystal grains. Consistent with other reports, we found that such artificially made grain boundaries are not always straight, but instead meander along the path of the underlying straight substrate boundary. Although we demonstrated some measure of control over the mean amplitude and wavelength of the meander (each is ≈200-800 nm), our recent breakthrough in the fabrication of bulk bicrystal boundaries in Y-123 has virtually eliminated meandering on all, except atomic, length scales. Their J_c values exhibit a similarly strong, exponential θ-dependence. What is particularly difficult to understand is the 30-times-lower magnitude of J_c on such 'perfect' bulk grain boundaries. A plausible explanation, based on differences of the pinning of Josephson vortices in these types of grain boundaries, is proposed here.

High-resolution transmission electron microscopy reveals no essential differences on the atomic scale between the bulk and bicrystal boundaries except the aforementioned meander. To explain the factor of 30 in J_c, we considered details of the dissipation at grain-boundary junctions. In long junctions, Josephson vortices can be created by the self-field of the transport current and lie within the junction (grain boundary) plane, perpendicular to its longer edges. Their size λ_j, along the boundary is defined by the falloff of the supercurrent and is related to J_{cj}, the intrinsic Josephson critical current density, i.e., that for an identical barrier with linear dimensions $L<<\lambda_j$. For long junctions, dissipation occurs when Josephson vortices move along the junction in response to the Lorentz force of any transport current through the junction. The ability to carry a supercurrent in long junctions ($L>>\lambda_j$) depends on pinning of Josephson vortices, and pinning of coreless Josephson vortices is optimized by defects of size $\approx\lambda_j$ along the junction (i.e., grain boundary meander).

The depinning critical current density is $J_{cp} = 4\,\alpha\, J_{cj}/\pi$, where α (≤ 1) reflects the actual sample-dependent pinning strength. Thus, the J_c for depinning Josephson vortices is proportional to J_{cj}. However, in the absence of pinning, or in the weak-pinning limit, dissipation occurs as soon as the self-field of the transport current J exceeds H_{c1} and flux enters. Then $J_{c1}\sim\sqrt{J_{cj}}$. Evidence for weak pinning in the bulk boundaries is compelling: it is also consistent with the absence of meandering and the linear decrease of I_c with applied field, which quantitatively predicts the correct sample sizes and allows the important conclusion that $\lambda_j \approx 0.5$ μm at 77 K for the 25° bulk boundary.

For thin-film boundaries, the width-to-thickness ratios are ≈100 (more generally in the range of 20-500), and stray fields (e.g., the earth's) are magnified at the film edges by that ratio. It is likely that H_{c1} at the film edges is exceeded before

current is applied, and thus depinning of Josephson vortices is relevant for film boundaries. Interpreting our data on a 24° boundary in that way provides $\lambda_j \approx 0.7\ \mu m$.

We now show a quantitatively plausible scenario linking all such measurements. It uses an effective pinning strength of $\alpha \approx 0.12$ for thin-film boundaries and the weak-pinning limit for the bulk boundaries. For a reasonable approximation to the data, we choose a simple form for $J_{cj}(\theta)$ and simple interpolations to the $\theta = 0$ limit. Figure 8 shows, within scatter, a very reasonable fit of this model to the relative magnitudes and θ-dependencies of almost all the grain-boundary J_c data.

In conclusion, we have presented a plausible flux-pinning model to explain the otherwise puzzling differences in J_c shown in Fig. 8 for bulk and thin-film bicrystal boundary types. This explanation provides guidelines for desirable grain-boundary properties in various situations. Meandering is highly desirable for biaxially textured, coated-conductor applications to enhance J_c. However, studies of the intrinsic J_{cj}, e.g., the effects of d-wave superconductivity, virtually require planar boundaries to avoid potentially large variations in J_{cj} and in the unknown α.

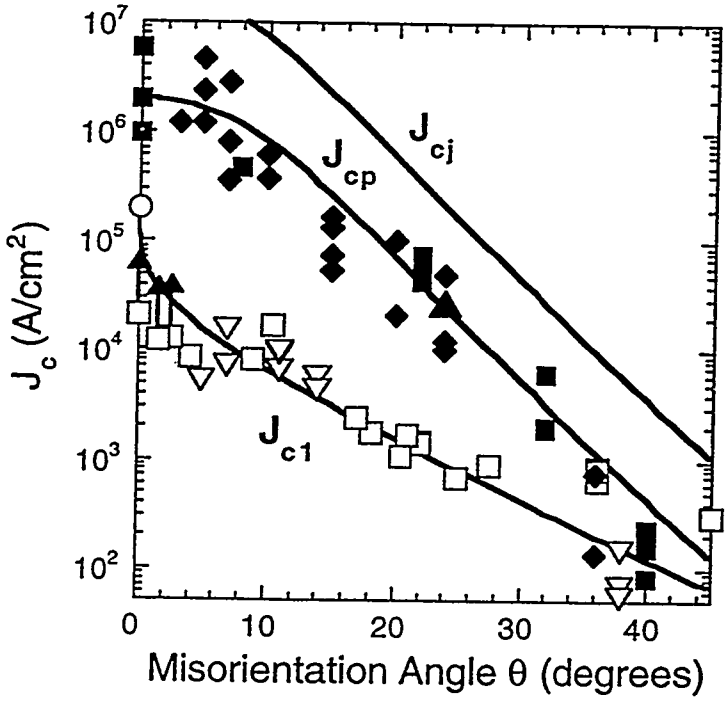

Fig. 8. Experimental data and model fits for J_{c1}, J_{cp}, and J_{cj} for Y-123 grain boundary.

HTS Flux Pump SBIR Project with Ability Engineering Technology

The high-T_c superconductor (HTS) flux pump primary, secondary, and inductive-load coils have been constructed (Fig. 9). The load coil was assembled with an iron yoke and has been operated at 77 K in liquid N_2 at currents to 125 A. The 77 K resistances of representative 10-tape PIT conductor section splice joints have been measured. The recovery characteristics, i.e., resistance with applied field and time to recover, of HTS conductors in the magnetic-switch environment have been measured. The test dewar and temperature control system have been assembled and operated successfully under flux-pump design conditions. The flux pump, load-coil assembly, and the magnetic-switch assembly are being integrated structurally and electrically. System evaluations are to follow.

Interactions

Balu Balachandran attended and presented a talk at the DOE Wire Workshop, St. Petersburg, FL, Jan. 29-30, 1998.

Balu Balachandran presented a seminar at the University of Wollongong, Australia, Feb. 5, 1998, entitled "Processing of Ag-Clad BSCCO Tapes."

Balu Balachandran, Steve Dorris, Nazarali Merchant, and Dean Miller participated and presented papers at the HTS symposium during the TMS Annual Meeting, San Antonio, TX, Feb. 16-18, 1998.

Dr. Shiming Wu, recently of Cambridge University, visited on February 16-20. She presented a seminar and discussed with several staff members her recent work on Ag-clad conductors.

Balu Balachandran met with Jim Daley, DOE, Washington, DC, for programmatic discussions on March 5, 1998.

Balu Balachandran presented a seminar at the National Research Institute for Metals (NRIM), Tsukuba, Japan, March 16, 1998, entitled "High-T_c Superconductors for Electric Power Applications: Current Status."

Balu Balachandran presented a seminar at the International Superconductivity Technology Center (ISTEC), Tokyo, March 17, 1998, entitled "Superconductivity Partnership Initiative (SPI): Current Status."

Balu Balachandran attended the NATO-sponsored HTS symposium in Moscow, Russia, during March 24-27, 1998.

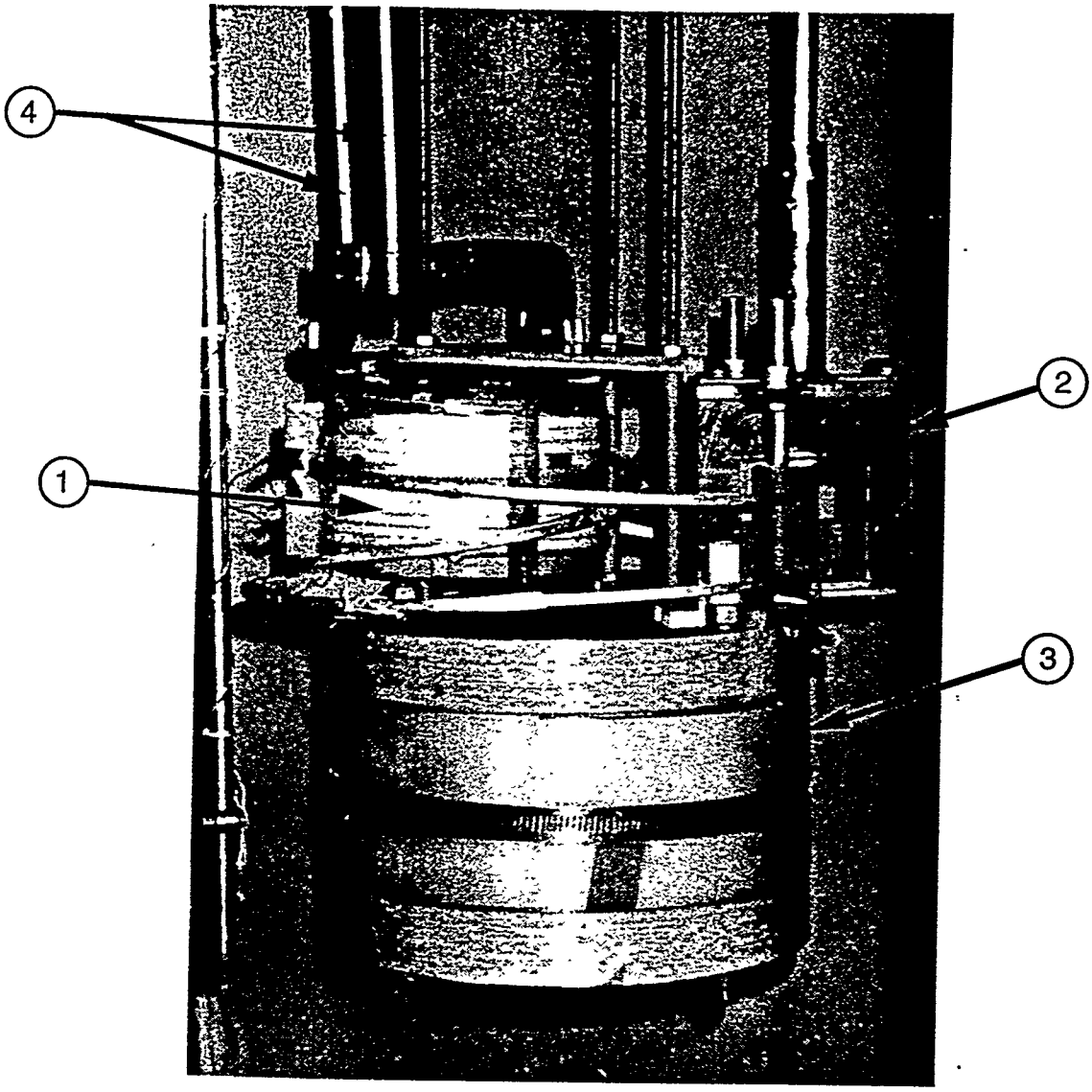

HTS Flux Pump Test Assembly; (1) Flux pump, (2) Magnetic-switch assembly, (3) Load coil, (4) Current leads to ambient.

Fig. 9. HTS flux pump unit with key components identified.

On March 27, Ken Goretta served as a member of Dr. Wangshui Wei's Ph.D. defense committee at Florida State University. Discussions on current and future work were also held with Dr. Justin Schwartz and his colleagues.

Balu Balachandran attended the High Energy Physics–LTS/HTS Workshop, Napa, CA, March 30-31.

List of Publications

Published:

J. P. Singh and N. Vasanthamohan, Effect of Sintering Temperature and Cooling Rate on Microstructure, Phase Formation, and Critical Current Density of Ag-Sheathed $Bi_{1.8}Pb_{0.4}Sr_2Ca_3O_x$ Superconducting Tapes, J. Mater. Res., Vol. 13, No. 2, Feb. 1998, pp. 261-268.

W. Wong-Ng and L. P. Cook, (NIST) F. Jiang and W. Greenwood (U. of Maryland), U. Balachandran and M. T. Lanagan, Subsolidus Phase Equilibria of Coexisting High-T_c Pb-2223 and 2212 Superconductors in the (Bi,Pb)-Sr-Ca-Cu-O System under 7.5% O_2, J. Mater. Res., Vol. 12, No. 11 (Nov. 1997), pp. 2855-2865.

W. Wei, J. Schwartz (Natl. High Magnetic Field Lab.), K. C. Goretta, U. Balachandran, and A. Bhargava (U. of Queensland), Effects of Nanosize MgO Additions to Bulk $Bi_{2.1}Sr_{1.7}CaCu_2O_x$, Physica C, Vol. 298 (1998), pp. 279-288.

Y. S. Cha, Z. J. Yang, L. R. Turner, and R. B. Poeppel, Analysis of a Passive Superconducting Fault Current Limiter, IEEE Transactions on Applied Superconductivity, Vol. 8, No. 1 (March 1998), pp. 20-25.

Submitted:

U. Balachandran, Recent Advances in the Development of High-T_c Superconductors for Electric Power Applications, INVITED paper for publication as a Special Article in Intl. Superconductivity Technology Center (ISTEC) Journal.

W. Wei, J. Schwartz (National High Magnetic Field Lab.), K. C. Goretta, U. Balachandran, and A. Bhargav (U. of Queensland), Effects of Nanophase MgO Additions on the Properties of $Bi_2Sr_2CaCu_2O_x$, Abstract presented at 127th Ann. Mtg. and Exhibition, TMS, San Antonio, Feb. 15-19, 1998.

S. P. Athur, P. Putman (Texas Center for Superconductivity), U. Balachandran, and K. Salama (Texas Center for Superconductivity), Melt-Processing of Yb-123 Tapes Coated on Silver Substrate, Abstract presented at 127th Ann. Mtg. and Exhibition, TMS, San Antonio, Feb. 15-19, 1998.

S. Sailb, A. N. Iyer, C. Vipulanandan, K. Salama (Texas Center for Superconductivity), and U. Balachandran, Electromechanical Characterization of Silver-Clad BSCCO Superconductors, Abstract presented at 127th Ann. Mtg. and Exhibition, TMS, San Antonio, Feb. 15-19, 1998.

U. Balachandran, High-T_c Superconductors for Electric Power Applications, Abstract of INVITED paper presented at 127th Ann, Mtg. and Exhibition, TMS, San Antonio, Feb. 15-19, 1998.

S. E. Dorris, N. Ashcom, T. Truchan, N. Merchant, and V. A. Maroni, Effects of Lead Content on Microstructure Development and Properties of Bi-2223 Powder-in-Tube Conductors, Abstract of paper presented at 127th Ann, Mtg. and Exhibition, TMS, San Antonio, Feb. 15-19, 1998.

U. Balachandran, V. Selvamanickam (IGC), P. Haldar (IGC), M. Lelovic (U. of Pittsburgh), and N. G. Eror (U. of Pittsburgh), Development of Ag-Clad Bi-2223 Superconductors for Electric Power Applications, Invited abstract of paper presented at Symp. on Processing and Critical Current of HTS, Wagga Wagga, Australia, Feb. 2-4, 1998.

R. L. Thayer, S. R. Schmidt, S. E. Dorris, B. L. Fisher, M. T. Lanagan, and J. W. Bullard (U. of IL-Champaign), Phase Formation and Densification of (Bi,Pb)-Sr-Ca-Cu-O (2223) Current Leads, Abstract of paper to be presented at 100th Ann. Mtg. of the American Ceramic Society, Cincinnati, May 3-6, 1998.

U. Balachandran, Development of High-T_c Superconductors for Electric Power Applications, Abstract to be presented at 100th Ann. Mtg. of Am. Ceram. Soc., Cincinnati, May 3-6, 1998.

U. Balachandran, Recent Advances in Fabrication of High-T Superconductors for Electric Power Applications, Invited abstract presented at NATO Advanced Research Intl. Workshop on High-Temperature Superconductors and Novel Inorganic Materials Engr., Moscow, March 24-29, 1998.

N. Vasanthamohan, J. P. Singh, D. Ebner, and K. A. Lubke, Improving the Transport Properties of Ag-Sheathed BSCCO (2223) Tapes by Optimizing the Cooling Procedure, Abstract to be presented at 100th Ann. Mtg. of the American Ceramic Society, Cincinnati, May 3-6, 1998.

U. Balachandran, V. Selvamanickam, P. Haldar (IGC), M. Lelovic, and N. G. Eror (U. of Pittsburgh), Development of Ag-Clad Bi-2223 Superconductors for Electric Power Applications, Invited paper presented at Symp. of Processing and Critical Current of HTS, Wagga Wagga, Australia, Feb. 2-4, 1998.

U. Balachandran, M. Lelovic, N. G. Eror (U. of Pittsburgh), and P. Haldar (IGC), Advances in Processing of Ag-Sheathed $(Bi,Pb)_2Sr_2Ca_2Cu_3Ox$ Superconductors, Invited paper submitted for publication in Proc. Third Pacific Rim Intl. Conf. on Advanced Materials and Processing, Honolulu, July 12-16, 1998.

M. P. Chudzik, M. Lanagan, R. Erck, and C. R. Kannewurf (Northwestern U.), Deposition of Biaxially Textured YSZ by Ion-Beam-Assisted Deposition, Abstract to be presented at 1998 Applied Superconductivity Conf., Palm Desert, Sept. 13-18, 1998.

S. Sagar, K. Lahiri, D. Shi (U. of Cincinnati), and Z. J. Yang, Effect of Sample Geometry on Levitation Force in Seeded-Melt-Processed $YBa_2Cu_3O_x$, To be published in IEEE Trans. on Magnetics.

A. Gupta (Northern Illinois U.), T. Mulcahy, J. Hull, and R. Abboud (Commonwealth Res. Corp.), Vibration Analysis of Composite Disks, Paper presented at 16th Intl. Modal Analysis Conf., Santa Barbara, CA, Feb. 2-5, 1998, sponsored by Soc. for Experimental Mechanics (SEM).

A. Gupta (Northern Illinois U.), T. M. Mulcahy, J. R. Hull, and R. G. Abboud (Commonwealth Res. Corp.), Vibration Analysis of Composite Disks, Abstract of paper presented at 16th Intl. Modal Analysis Conf., Santa Barbara, CA, Feb. 2-5, 1998, sponsored by Soc. for Experimental Mechanics (SEM).

T. A. Deis, M. Lelovic, N. G. Eror, and U. Balachandran, Effect of Ag Doping on Structure and Critical Temperature of $Bi_2Sr_2CaCu_2O_{8+\delta}$ Superconductors, Submitted to Applied Superconductivity (Jan. 1998).

Y. S. Cha and T. R. Askew (Kalamazoo College), Transient Response of a High-Temperature Superconductor Tube to Pulsed Magnetic Fields, Submitted to Physica C (Feb. 1998).

L. R. Turner and M. W. Foster, Optimizing Flux Exclusion to Model Hysteretic Force History in HTS, Extended abstract to be presented at CEFC (Computational Electromagnetic Field Conf.), Tucson, June 1-3, 1998.

1996-8 Patents:

Mixed-Mu superconducting bearings
John R. Hull and Thomas M. Mulcahy
U.S. Patent No. 5,722,303 (Mar. 3, 1998).

Synthesis of increased-density bismuth-based superconductors with cold isostatic pressing and heat treating
Michael T. Lanagan, John J. Piccolo, and Stephen E. Dorris
U.S. Patent 5,674814 (October 7, 1997); report ANL–IN–93–058.

Near net shape forming of continuous lengths of superconducting wire
Stephen Danyluk, Michael McNallan, Robert Troendly, Roger B. Poeppel, Kenneth C. Goretta, and Michael T. Lanagan
U.S. Patent 5,661,113 (August 26, 1997); report ANL–IN–93–054.

Method for obtaining large levitation pressure in superconducting magnetic bearings
John R. Hull
U.S. Patent No. 5,654,683 (Aug. 5, 1997).

Low-loss, high-speed high-T_c auperconducting bearings
John R. Hull, Thomas M. Mulcahy, and Kenneth L. Uherka
U.S. Patent No. 5,640,887 (June 24, 1997).

Seed crystals with improved properties for melt processing superconductors for practical applications
Boyd W. Veal, Arvydas P. Paulikas, and Uthamalingham Balachandran
U.S. Patent 5,611,854 (March 18, 1997); report ANL–IN–94–123.

High temperature superconducting fault current limiter
John R. Hull
U.S. Patent No. 5,600,522 (Feb. 4, 1997).

Method for harvesting single crystals from a peritectic melt
Volker R. Todt, Suvankar Sengupta, and Donglu Shi
U.S. Patent 5,549,748 (August 27, 1996); report ANL–IN–93–130b.

Method of producing improved microstructure and properties for ceramic superconductors
Jitendra P. Singh, Rob A. Guttschow, Joseph T. Dusek, and Roger B. Poeppel
U.S. Patent 5,525,586 (June 11, 1996); report ANL–IN–91–072.

Method for harvesting rare earth barium copper oxide single crystals
Volker R. Todt, Suvankar Sengupta, and Donglu Shi
U.S. Patent 5,504,060 (April 2, 1996); report ANL–IN–93–130.

Rapid formation of phase-clean 110 K (Bi-2223) powders derived via freeze-drying process
Uthamalingham Balachandran and Nicholas G. Eror
U.S. Patent 5,523,285 (June 4, 1996); report ANL–IN–93–052.

Process of preparing superconductors
Stephen E. Dorris, D. A. Burlone (BASF), and C. W. Morgan (BASF)
DOE Case No. S-82,194; report ANL–IN–94–090, application filed July 19, 1995.

Surface texturing of superconductors by controlled oxygen pressure
Nan Chen, Kenneth C. Goretta, and Stephen E. Dorris
Serial No. 08/649,865; report ANL–IN–96–052, application filed May 10, 1996.

Automatic HTS force measurement instrument
Scott T. Sanders and Ralph C. Niemann; report ANL–IN–96–077, application filed April 10, 1997.